Resonances, Instabilities, and Structure Selection of Driven Josephson Lattice in Layered Superconductors

A. E. Koshelev and I. S. Aranson
Materials Science Division, Argonne National Laboratory, Argonne, Illinois 60439
(Received 11 July 2000)

We investigate the dynamics of the Josephson vortex lattice in layered high-T_c superconductors at high magnetic fields. It is shown that the average electric current depends on the lattice structure and is resonantly enhanced when the Josephson frequency matches the frequency of the plasma mode. We find the stability regions of a moving lattice. It is shown that a specific lattice structure at a given velocity is uniquely selected by the boundary conditions; at small velocities a periodic triangular lattice is stable and looses its stability at some critical velocity. At even higher velocities, a structure close to a rectangular lattice is restored.

PACS numbers: 74.60.Ge, 47.54.+r, 74.50.+r

Transport properties of layered superconductors, such as $Bi_2Sr_2CaCu_2O_x$ (BSCCO), in magnetic field parallel to the layers are determined by the dynamics of Josephson vortex lattice (JVL) [1–3]. Moving JVL generates a traveling electromagnetic wave in the medium. Similar to the Eck resonance in a single junction [4], one expects a strong resonance emission when the velocity of the lattice matches the plasma wave velocity [5,6]. In the current-voltage (I-V) dependence this resonance is seen as a strong enhancement of current at fixed voltage. In contrast to a single junction, JVL in layered superconductors has soft degrees of freedom related to the phase shifts between different layers. This leads to a rich variety of dynamic states observed in numerical simulations [7]. In particular, a periodic lattice corresponds to a constant phase shift between neighboring layers, ranging from 0 for the rectangular lattice to π for the static triangular lattice. The moving lattice generates an electromagnetic wave with the c-axis wave vector selected by the lattice structure. Since the velocity of a plasma wave propagating along the layers depends on this wave vector [8], *the resonant velocity of the lattice depends on its structure*.

In this Letter, we investigate the stability of moving JVLs and the evolution of structure as a function of its velocity for large size samples [9]. We show that a specific lattice structure at a given velocity is uniquely selected by the boundary conditions. At small velocities a periodic lattice is stable. The phase shift between neighboring layers smoothly decreases with the increase of velocity, starting from π for a static lattice. At some critical velocity the lattice becomes unstable. At even higher velocities a periodic lattice with the phase shift smaller than $\pi/2$ is restored again.

Consider a layered superconductor in a magnetic field applied along the layers (y axis) with transport current flowing across the layers (z axis). The dynamics of such a system is described by the inductively coupled sine-Gordon equations for the gauge-invariant phase differences θ_n [10]. Introducing the reduced time $\tau = \omega_p t$ and in-plane coordinate $u = x/(\gamma s)$, we express currents $j_{x,n}$, $j_{z,n}$ and electric fields $E_{z,n}$ via θ_n and the reduced magnetic fields $h_n = H_n 2\pi\gamma\lambda_{ab}^2/\Phi_0$ as

$$j_{z,n} = j_J(\sin\theta_n + \nu_{ab}\partial\theta_n/\partial\tau), E_{z,n} \approx E_p\partial\theta_n/\partial\tau\,,$$

$$j_{x,n+1} - j_{x,n} = j_{ab}\left(1 + \nu_{ab}\frac{\partial}{\partial\tau}\right)\left(\frac{\partial\theta_n}{\partial u} - \frac{h_n}{l^2}\right),$$

where ω_p is the Josephson plasma frequency, γ is the anisotropy factor, s is the interlayer spacing, j_J is the Josephson current, $E_p \equiv \Phi_0\omega_p/(2\pi cs)$, $l = \lambda_{ab}/s$, and $j_{ab} \equiv c\Phi_0/(8\pi\lambda_{ab}^2\gamma s)$. $\nu_c = 4\pi\sigma_c/(\varepsilon_c\omega_p)$ and $\nu_{ab} = 4\pi\sigma_{ab}\lambda_{ab}^2\omega_p/c^2$ are the dissipation parameters, which are determined by the quasiparticle conductivities σ_c and σ_{ab} and are connected as $\nu_c/\nu_{ab} = \sigma_c\gamma^2/\sigma_{ab}$. Using the above relations we derive from the Maxwell equations the coupled equations for θ_n and h_n

$$\frac{\partial^2\theta_n}{\partial\tau^2} + \nu_c\frac{\partial\theta_n}{\partial\tau} + \sin\theta_n - \frac{\partial h_n}{\partial u} = 0\,, \tag{1}$$

$$\left(\nabla_n^2 - \frac{1}{l^2}\right)h_n + \frac{\partial\theta_n}{\partial u} + \nu_{ab}\frac{\partial}{\partial\tau}\left(\frac{\partial\theta_n}{\partial u} - \frac{h_n}{l^2}\right) = 0\,, \tag{2}$$

where $\nabla_n^2 h_n \equiv h_{n+1} + h_{n-1} - 2h_n$. Equivalent forms of these equations have been derived in Refs. [6,11]. In the case of negligible in-plane dissipation ($\nu_{ab} = 0$) they can be reduced to equations containing only θ_n [10]. Taking parameters typical for underdoped BSCCO at $T \approx 50$ K: $\gamma = 500$, $\lambda_{ab} = 240$ nm, $s = 15$ Å, $\sigma_{ab} = 2 \times 10^4\ [\Omega\cdot\mathrm{cm}]^{-1}$, and $\sigma_c = 2 \times 10^{-3}\ [\Omega\cdot\mathrm{cm}]^{-1}$, one obtains estimates: $\nu_{ab} \approx 0.1$ and $\nu_c \approx 0.002$, which we will use in numerical computations. For these parameters the dissipation in a wide range of electric and magnetic fields is mainly determined by the in-plane channel [12].

We consider the situation when all junctions are filled by JVs. This is always the case at high magnetic field B above $\Phi_0/5.5\gamma s^2$ [13] or at high currents, when all junction are driven into the resistive state. Neglecting self-field of the

 0031-9007/00/85(18)/3938(4)$15.00

transport current, we represent a solution to Eqs. (1) and (2) for the resistive state in the form

$$\theta_n(\tau,u) = \omega_E\tau + k_H u + \phi_n(\tau) + \tilde{\theta}_n(\tau,u), \quad (3)$$

$$h_n(\tau,u) = h + \tilde{h}_n(\tau,u). \quad (4)$$

Here the Josephson frequency ω_E is determined by the electric field, $\omega_E = E_z/E_p$, and the wave vector k_H is determined by the magnetic field, $k_H = 2\pi H\gamma s^2/\Phi_0 = h/l^2$. $\tilde{\theta}_n(\tau,u)$ and $\tilde{h}_n(\tau,u)$ are the oscillating phase and magnetic field induced by Josephson coupling, $\tilde{\theta}_n$, $\tilde{h}_n \propto \sin(\omega_E\tau + k_H u + \alpha_n)$. Solution (3) corresponds to the lattice moving with velocity ω_E/k_H. The structure of the lattice is determined by the phase shifts ϕ_n. Without Josephson coupling the system is degenerate with respect to arbitrary phase shifts ϕ_n. Josephson coupling eliminates this degeneracy. It either leads to slow dynamics of phase shifts ϕ_n or selects a certain steady state structure. The equations for $\phi_n(\tau)$ can be obtained using an expansion with respect to Josephson coupling and averaging over fast degrees of freedom. This procedure will be described in detail elsewhere [14].

For periodic JVL one has $\phi_n = \kappa n$. In such a state the chains of JVs in the neighboring layers are shifted by the fraction $\kappa/2\pi$ of the lattice constant (see inset in Fig. 1). In particular, $\kappa = 0$ corresponds to a rectangular lattice, and $\kappa = \pi$ corresponds to a triangular lattice (ground state at $\omega_E = 0$). In the first order with respect to Josephson current, the oscillating phase $\tilde{\theta}_n$ is given by $\tilde{\theta}_n = \mathrm{Im}\{\mathcal{G}(\kappa)\exp[i(\omega_E\tau + k_H u + \kappa n)]\}$ with

$$\mathcal{G}(\kappa) = \left[\omega_E^2 - i\nu_c\omega_E - \frac{k_H^2(1 + i\nu_{ab}\omega_E)}{2(1-\cos\kappa) + (1 + i\nu_{ab}\omega_E)/l^2}\right]^{-1}.$$

To the second order we obtain the average reduced Josephson current $i_J \equiv i_J(\kappa, k_H, \omega_E) = \langle\sin\theta_n(\tau,u)\rangle$ [11]. In the case of not very large in-plane dissipation $\nu_{ab}\omega_E \ll 2l^2(1-\cos\kappa) + 1$, it has the resonant dependence on the Josephson frequency ω_E (electric field)

$$i_J = \frac{1}{2}\frac{\omega_E\nu(\kappa)}{[\omega_E^2 - \omega_p^2(\kappa)]^2 + [\omega_E\nu(\kappa)]^2},$$

where $\omega_p(\kappa) = k_H[2(1-\cos\kappa) + \frac{1}{l^2}]^{-1/2}$ is the plasma frequency at the wave vector κ and

$$\nu(\kappa) \equiv \nu_c + \frac{2(1-\cos\kappa)k_H^2\nu_{ab}}{[2(1-\cos\kappa) + 1/l^2]^2}$$

is the dissipation parameter of the plasma mode [11]. When the frequency ω_E matches the corresponding plasma wave frequency $\omega_p(\kappa)$, a resonance enhancement of the current is expected. The moving lattice generates a traveling electromagnetic wave with the Poynting vector $\mathbf{P}$. For the in-plane component of $\mathbf{P}$ we obtain

$$P_x \approx \frac{P_{ab}\omega_E\omega_p^2(\kappa)/k_H}{[\omega_E^2 - \omega_p^2(\kappa)]^2 + [\omega_E\nu(\kappa)]^2}, \qquad P_{ab} = \frac{\Phi_0^2\omega_p}{32\pi^3\lambda^2 s\gamma}. \quad (5)$$

For typical BSCCO parameters at low temperatures ($\lambda =$ 200 nm, $\gamma = 500$, $\omega_p/2\pi = 150$ GHz) we obtain $P_{ab} \approx$ 125 W/cm^2.

To investigate the stability of JVL we perturb the lattice solution as $\phi_n(\tau) = \kappa n + \mathrm{Re}\{u_q\exp[\alpha(q)\tau + iqn]\}$ and derive from Eqs. (1) and (2) the eigenvalue $\alpha(q) \equiv \alpha(q,\kappa,k_H,\omega_E)$

$$\alpha(q) = -\frac{1}{4}\frac{\mathcal{G}(\kappa+q) + \mathcal{G}^*(\kappa-q) - 2\mathrm{Re}[\mathcal{G}(\kappa)]}{\nu_c + \frac{1}{4i}[\mathcal{F}(\kappa+q,\kappa) - \mathcal{F}^*(-\kappa+q,\kappa)]} \quad (6)$$

with

$$\mathcal{F}(q,q_1) \equiv \left[-2\omega_E + i\nu_c + \frac{ik_H^2\nu_{ab}}{2(1-\cos q) + \frac{1+i\nu_{ab}\omega_E}{l^2}}\frac{2(1-\cos q_1)}{2(1-\cos q_1) + \frac{1+i\nu_{ab}\omega_E}{l^2}}\right]\mathcal{G}(q)\mathcal{G}(q_1).$$

The lattice is stable if there is no exponentially growing solution in the whole q interval, i.e., $\mathrm{Re}[\alpha(q)] \le 0$, for $0 \le q \le \pi$. The onset of instability is characterized by the wave vector q_i of the most unstable mode. There are three special cases: the long-wave instability $q_i = 0$, the short-wave instability $q_i = \pi$, and the instability with $0 < q_i < \pi$. One can also distinguish absolute and convective instabilities [15]. The spectrum $\alpha(q)$ has an important symmetry property $\alpha(q = \pi, \kappa = \pi/2) = 0$. This means that a stable region cannot cross the line $\kappa = \pi/2$ and *it is impossible to evolve continuously from the*

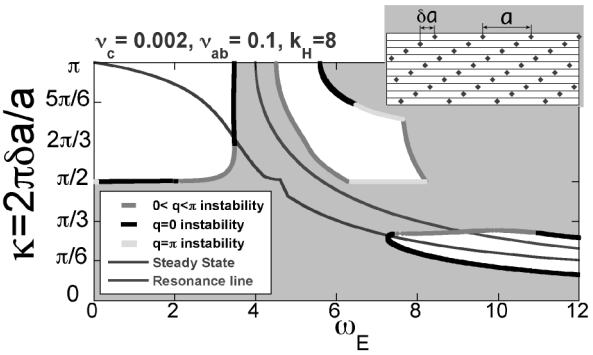

FIG. 1. Stability regions of moving Josephson lattice in the plane ω_E-κ calculated for representative parameters $\nu_c = 0.002$, $\nu_{ab} = 0.1$, and $k_H = 8$. Grey regions correspond to unstable lattices. Sections of the boundaries marked by black correspond to the long-wave instability. Sections marked by light grey correspond to the instability with $q = \pi$. The line starting at (0, π) shows the dependence of the lattice wave vector on the frequency ω_E selected by the boundary with free space. We also show the resonance line, corresponding to matching between the Josephson frequency and the frequency of the plasma wave at the wave vector κ. The inset sketches a steady state corresponding to a regular lattice.

static triangular lattice to the fastly moving rectangular lattice without intersecting an instability boundary. The triangular lattice always looses its stability before reaching the resonance $\omega_E = k_H/2$, at the frequency $\omega_\Delta(k_H)$ which is determined by a simple analytical equation $\omega_\Delta^2 - \frac{k_H^2}{4} = -\omega_\Delta(\nu_c + \frac{k_H^2\nu_{ab}}{4})(\sqrt{1 + \nu_{ab}^2\omega_\Delta^2} - \nu_{ab}\omega_\Delta)$.

To explore the stability of JVL we calculated numerically $\mathrm{Re}[\alpha(q)]$ (6) throughout the $\omega_E - \kappa$ plane and found the lines at which either $\mathrm{Re}[\alpha(q)] = 0$ at finite q or $\mathrm{Re}[d^2\alpha(q)/dq^2] = 0$ at $q = 0$. The stability diagram for representative parameters $\nu_c = 0.002$, $\nu_{ab} = 0.1$, and $k_H = 8$ is shown in Fig. 1. For these parameters we found three stability regions at moderate ω_E: (i) the low-velocity region located below the resonance line and at $\pi/2 < \kappa < \pi$, (ii) the high-velocity region located along the resonance line with κ approaching 0 with an increase of ω_E, and (iii) the region located above the resonance line and at $\pi/2 < \kappa < \pi$ (this region disappears at higher fields). At the boundary of the first region the lattice experiences a long-wave instability for $\kappa > 2.04$. At smaller κ the instability occurs at finite wave vector $q = q_i$ and q_i grows continuously with the decrease of κ.

Selection by the system of a specific wave number κ from the continuous spectrum is not directly related to stability of the corresponding periodic structure. For the static case the structure is selected by the minimum energy condition. Such a condition is absent in the dynamic case. In this case a specific JVL structure can be determined by the boundary. To demonstrate this, we consider a semi-infinite stack of junctions with $n = 1, 2, \ldots$ separated by a sharp boundary from the medium with arbitrary electromagnetic properties. To derive equations for the phase shifts ϕ_n for such a system we have to find a solution of the linear equations without Josephson coupling, taking into account the boundary conditions. For plasma wave with given frequency $\omega = \omega_E$ and wave vector along the layers $k = k_H$ the oscillating phases ($\tilde{\theta}_n$) and magnetic fields ($\tilde{h}_n$) in the junctions can be written as

$$\tilde{\theta}_n, \tilde{h}_n \propto \exp(-iq_+n) + \mathcal{B}\exp(iq_+n), \quad \text{at } n \geq 1, \quad (7)$$

where $q_+ \equiv q_+(k, \omega)$ is a (complex) wave vector given by

$$\cos q_+ = 1 - \frac{k^2(1 + i\nu_{ab}\omega)}{2(\omega^2 - i\nu_c\omega)} + \frac{1 + i\nu_{ab}\omega}{2l^2}, \quad (8)$$

with $\mathrm{Im}[q_+] > 0$. The properties of the boundary are completely characterized by the complex amplitude of reflected wave $\mathcal{B} \equiv \mathcal{B}(k, \omega)$, which has to be found by matching the solution (7) with electromagnetic oscillations in the medium at $z < 0$. In general, $\mathcal{B}(k, \omega)$ can be a complex number with an arbitrary absolute value. Only in the simplest case of vanishing dissipation and propagating wave [$\mathrm{Im}(q_+) = 0$], $\mathcal{B}(k, \omega)$ determines a conventional reflection coefficient, $R(k, \omega) = |\mathcal{B}(k, \omega)|^2$, and has property $|\mathcal{B}(k, \omega)| < 1$. A large class of boundaries, including boundary with free space, is well described by the ideal reflection $\mathcal{B} = -1$. Averaging with respect to oscillating phases and field, we derive the following equation for the steady state phase shifts ϕ_n

$$\frac{1}{2}\sum_{m=1}^{\infty} \mathrm{Im}\{G(n, m)\exp[-i(\phi_n - \phi_m)]\} = i_J, \quad (9)$$

where

$$G(n, m) = G_0(n - m) + \mathcal{B}G_0(n + m), \quad (10)$$

$$G_0(n) \equiv G_0(n; k_H, \omega_E) = \frac{\delta_n}{\omega_E^2 - i\nu_c\omega_E} - \frac{k_H^2(1 + i\nu_{ab}\omega_E)}{(\omega_E^2 - i\nu_c\omega_E)^2}\frac{\exp iq_+|n|}{2i\sin q_+}. \quad (11)$$

The second term in Eq. (10) describes the surface contribution and vanishes at $n, m \to \infty$. The solution, corresponding to the lattice in the bulk, has the form $\phi_n = \kappa n + u_n$, where u_n is the surface deformation, $u_n \to 0$ at $n \to \infty$. Substituting this ansatz into Eq. (9) we obtain a nonlinear degenerate system of equations for u_n. The solution for u_n exists only for special values of κ, i.e., *the bulk structure is selected by the boundary conditions*. For such selected states z component of the Poynting vector P_z is always directed from the boundary towards the bulk of the sample [16]. A similar pattern selection mechanism is relevant for various nonequilibrium systems [17]. At small ω_E the system becomes linear with respect to u_n and its solvability condition can be found analytically. In the case $\mathcal{B} = -1$ we obtain deformation of the lattice at small velocities $\kappa \approx \pi - (\nu_{ab} + 7\nu_c/k_H^2)\omega_E$. In a finite system with identical boundaries the configuration is

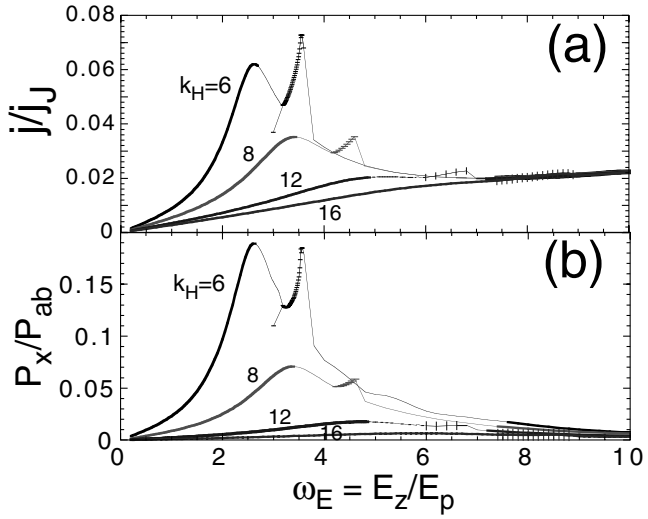

FIG. 2. (a) Current-voltage characteristics at different magnetic fields, for $k_H = 6$, 8, 12, and 16 (for $\gamma = 500$ $H \approx k_H \cdot 0.3$T). The dependencies are obtained using numerically computed steady states with parameters $\nu_c = 0.002$, $\nu_{ab} = 0.1$. The thick lines show stable branches and the thin lines show unstable branches. The branches, marked by dashes, correspond to the double-periodic lattices. (b) Electric field dependencies of the Poynting vector along the layers for electromagnetic wave generated by the moving lattice [see Eq. (5)].

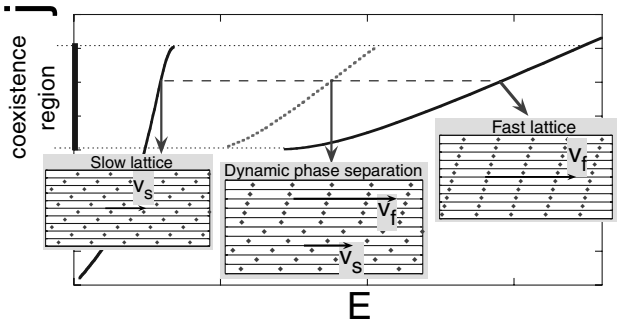

FIG. 3. Multibranch structure of the current-voltage characteristic due to dynamic phase separation. Two states corresponding to slow lattice motion (velocity v_s) and fast lattice motion (velocity v_f) coexist within the current range marked at the vertical axis. In this region the intermediate phase-separated states exist, in which the system is split into fastly and slowly moving regions. The intermediate branch corresponding to one of such states is shown by the dotted line.

typically symmetric because each boundary selects the same wave number. The waves collide in the middle forming a phase defect [17].

To find the steady state configurations at all velocities we solved Eq. (9) numerically taking $\mathcal{B} = -1$ and using the same parameters ($\nu_c = 0.002$, $\nu_{ab} = 0.1$). The dependence $\kappa(\omega_E)$ obtained from these solutions for $k_H = 8$ is shown in Fig. 1 together with the stability regions. At small velocities the lattice experiences smooth evolution of structure with the lattice wave vector κ decreasing from π at zero velocity to smaller values until it hits the instability boundary. At higher velocities the stable lattice with $\kappa < \pi/2$ is restored. The structure continues to evolve smoothly towards the rectangular configurations with an increase of velocity. Near the line $\kappa = \pi/2$ we observe a transition to the double-periodic lattice $\phi_n = \pi n/2 + (-1)^n v$, which becomes stable at high fields.

Figure 2 shows the evolution of the current-voltage dependence and the in-plane Poynting vector (5) with an increase of magnetic field. Up to magnetic field $H \approx \sqrt{\sigma_{ab}/(\gamma^2\sigma_c)}\,\Phi_0/(\pi\gamma s^2)$ ($k_H \approx 16$), the current-voltage dependencies have two stable branches, corresponding to moving periodic lattices, separated by a broad instability region where periodic JVL cannot exist. In this regime two lattice solutions exist within a finite range of currents. Such a coexistence is facilitated by the high in-plane dissipation, which causes a strong dependence of the JVL velocity on its structure. Within the coexistence region one can expect a family of intermediate states, in which the system is split into two (or more) domains moving with different velocities separated by a phase defect [dynamic phase separation; see Fig. 3]. The phase-separated states give the most natural interpretation of the multiple I-V branches observed by Hechtfischer *et al.,* who studied transport properties of JVL in BSCCO mesas at high magnetic fields [2]. This interpretation can be verified by measuring the spectrum of microwave irradiation emitted by the stack. Instead of a single peak located at the Josephson frequency corresponding to the average voltage, the spectrum of irradiation should contain two peaks corresponding to the "fast" and "slow" states.

In conclusion, we investigated the stability and boundary structure selection of the driven JVL. We found two major stability regions, separated by an unstable region: the low-velocity region corresponds to a moving structure close to a triangular lattice, and the high-velocity region corresponds to an almost rectangular lattice.

A. E. K. thanks R. Kleiner, N. F. Pedersen, M. Tachiki, and K. Gray for helpful discussions. This work was supported by the U.S. DOE, Office of Science under Contract No. W-31-109-ENG-38. A. E. K. also would like to acknowledge support from the JST (Japan) and to thank the National Research Institute for Metals for hospitality.

[1] J. U. Lee *et al.,* Appl. Phys. Lett. **67**, 1471 (1995); **71**, 1412 (1997).
[2] G. Hechtfischer *et al.,* Phys. Rev. Lett. **79**, 1365 (1997); Phys. Rev. B **55**, 14 638 (1997).
[3] Yu. I. Latyshev *et al.,* Physica (Amsterdam) **282C–287C**, 387 (1997); **293C**, 174 (1997).
[4] R. E. Eck, D. J. Scalapino, and B. N. Taylor, Phys. Rev. Lett. **13**, 15 (1964).
[5] T. Koyama and M. Tachiki, Solid State Commun. **96**, 367 (1995).
[6] S. N. Artemenko and S. V. Remizov, JETP Lett. **66**, 853 (1997).
[7] M. Machida *et al.,* Physica (Amsterdam) **330C**, 85 (2000); R. Kleiner *et al.,* Phys. Rev. B **62**, 4086 (2000).
[8] S. Sakai *et al.,* Phys. Rev. B **50**, 12 905 (1994).
[9] We do not consider resonances related to the finite-size effect (Fiske resonances). The Fiske resonant frequencies for layered superconductors have been classified by R. Kleiner, Phys. Rev. B **50**, 6919 (1994) and detected experimentally by A. Irie, Y. Hirai, and G. Oya, Appl. Phys. Lett. **72**, 2159 (1998).
[10] S. Sakai, P. Bodin, and N. F. Pedersen, J. Appl. Phys. B **73**, 2411 (1993); L. N. Bulaevskii *et al.,* Phys. Rev. B **50**, 12 831 (1994).
[11] L. N. Bulaevskii *et al.,* Phys. Rev. B **53**, 14 601 (1996).
[12] A. E. Koshelev, Phys. Rev. B **62**, R3616 (2000).
[13] L. N. Bulaevskii and J. R. Clem, Phys. Rev. B **44**, 10 234 (1991); M. Ichioka, Phys. Rev. B **51**, 9423 (1995).
[14] A. Koshelev and I. Aranson (to be published).
[15] For a convective instability a localized perturbation grows exponentially at some moving frame and decays at fixed point. For an absolute instability the perturbation grows at any fixed point, see, e.g., E. M. Lifshits and L. P. Pitaevskii, *Physical Kinetics* (Pergamon Press, Oxford, New York, 1981).
[16] The opposite case describes the scattering of the incoming wave generated far away from the boundary with the wave vector given by an external source (or opposite boundary). In this case the boundary does not select the structure in the bulk [17].
[17] M. C. Cross and P. C. Hohenberg, Rev. Mod. Phys. **65**, 851 (1993).